Universities Council on Water Resources
Journal of Contemporary Water Research & Education
Issue 175, Pages 1-14, April 2022

Understanding the Water Resources of a Mountain-block Aquifer: Tucson Mountains, Arizona

*Christopher J. Eastoe[1] and Kimberly R. Beisner[2]

[1]*Retired, Department of Geosciences, University of Arizona, Tucson, AZ*
[2]*U.S. Geological Survey, Albuquerque, NM*
**Corresponding author*

Abstract: Water resources are limited in arid locations such as Tucson Basin. Residential development in the Tucson Mountains to the west of Tucson, Arizona, is limited by groundwater resources. Groundwater samples were collected from fractured bedrock and alluvial aquifers surrounding the Tucson Mountains to assess water quality and recharge history through measurement of stable O, H, and S isotopes; tritium; and ^{14}C. Most groundwater is a mixture of different ages but is commonly several thousand years old. A few sampling locations indicated a component of water recharged after the above-ground nuclear testing of the mid 1950s, and these sites may represent locations near where the aquifer receives present-day recharge. The Tucson Mountains also host sulfide deposits associated with fractures and replacement zones; these locally contribute to poor-quality groundwater. Projections of future climate predict intensifying drought in southwestern North America. In the study area, a combination of strategies such as rainwater harvesting, exploitation of renewable water, and low groundwater use could be used for sustainable use of the groundwater supply.

Keywords: *groundwater, fractured rock, isotopes, recharge, residence time, water supply, Arizona*

Research Implications

- Groundwater in the Tucson Mountains occurs in poorly-connected rock fractures.
- Groundwater in caldera-complex volcanic rock is a mixture of late Pleistocene and pre-bomb, mainly summer recharge; little recharge occurs at present.
- Groundwater supply is limited, and of poor quality where affected by sulfide mineralization.
- Post-bomb recharge occurs in Oligocene volcanic rock and Cretaceous arkose, possibly providing a small, sustainable water supply.

The Tucson Mountains form the western boundary of the northern part of Tucson Basin in southeastern Arizona, USA (Figure 1). The Tucson metropolitan area occupies much of Tucson Basin, which is the alluvial basin to the east of the mountains, and has spilled over into Avra Valley, the alluvial basin to the west. The mountains and their foothills constitute a biodiverse landscape of the Sonoran Desert. Most of the mountain range and part of the adjacent foothills are protected within the Saguaro National Park and Pima County Parks. As Tucson has grown, private land adjacent to the parks, including some of the larger valleys within the hard-rock range, has attracted low-density urban development. Several of these areas are at present beyond the reach of existing water and wastewater infrastructure and must rely on private wells, rainwater collection, or hauling water for domestic water supply, and individual disposal systems for wastewater.

The demand for water in the settled part of the mountain range continues to grow at a time when some private well owners report falling groundwater levels (Robert Webb, retired U.S. Geological Survey, oral communication 2017). Arizona has experienced drought since about 2000 (Arizona Department of Water Resources 2020a), manifested in Tucson by decrease in winter

rainfall (e.g., Eastoe and Dettman 2016). In the arid southwestern USA, future climate change is expected to result in higher temperatures (USGCRP 2017) and prolonged drought due to decreasing winter rain as the jet stream and storm tracks move poleward (Udall and Overpeck 2017). Future warming may decrease groundwater recharge as evapotranspiration increases. Management of water resources in the Tucson Mountains and similar mountain ranges can be informed by an improved understanding of the mountain-block aquifers.

Isotope studies of rainwater and groundwater in Tucson Basin and surrounding mountain ranges have contributed much to the understanding of the hydrology of the basin, and to the understanding of regional recharge mechanisms (Kalin 1994; Eastoe et al. 2004; Gu 2005; Eastoe and Dettman 2016; Eastoe and Gu 2016; Eastoe and Towne 2018). In the Tucson Basin, these studies have identified long-term mean isotope compositions in local precipitation, isotope lapse rates with altitude, domains of groundwater of different sources in basin alluvium, zones of basin alluvium in which recharge occurs rapidly, and evolution of groundwater sources beneath downtown Tucson. At regional scale, the studies have proposed multiple recharge mechanisms that appear to be zoned with respect to basin location.

Studying the hydrology of mountain blocks is commonly challenging because of paucity of field data and difficulty of access to sample locations (Wilson and Guan 2004). At the small scale of mountain headwater catchments, tracer studies have been combined with hydrologic flux observations and in some cases with modeling to constrain the relation between precipitation, soil storage, and streamflow (e.g., Katsuyama et al. 2005; Aishlin and McNamara 2011; Ajami et al. 2011; Gabrieli et al. 2012; Dwivedi et al. 2019). Isotope tracers have been applied at the scale of mountain blocks to track groundwater movement within mountain blocks (Winograd et al. 1998; Earman 2004) and to identify mountain-block recharge (MBR) to surrounding lowland aquifers (James et al. 2000; Manning and Solomon 2004; Thiros and Manning 2004; Wahi et al. 2008; Harris et al. 2010; Newton et al. 2012; Eastoe and Rodney 2014). Eastoe and Wright (2019) examined the distribution of isotope tracers in mountain-block groundwater of the southern Basin-and-Range Province, identifying several recharge mechanisms that appear to depend on altitude and lithology. Modeling of mountain-block topography and permeability predicts the partitioning of recharge between base flow in mountain streams and MBR, and the relationship of MBR to depth of fractures and topography (Welch and Allen 2012; 2014). Ren et al. (2019) used borehole observations in an experimental well field in granite to estimate hydrologic apertures of fractures and local fracture porosity; they noted that groundwater flow would also depend on fracture connectivity.

In the case of the Tucson Mountains, groundwater can be sampled from numerous private supply wells that occur in clusters in the northern part of the mountain block, over an area of about 75 km^2. Eastoe and Wright (2019) published a small isotope dataset (stable O and H isotopes, tritium, and ^{14}C) for wells in hard rock of the Tucson Mountains, and concluded that groundwater recharge in the range occurred by a mechanism (to be explained in detail below) that is unusual in other mountain blocks of southern Arizona. Beisner and Gray (2018) published a second dataset (stable O and H isotopes, sulfate isotopes, Sr, tritium, and ^{14}C) for eight groundwater samples adjacent to the range front in a small area near the Old Yuma Mine (Area Y, Figure 1), with the aim of identifying contamination emanating from the mine workings. To these datasets can be added stable O and H measurements with a few tritium and ^{14}C measurements for wells completed in alluvium near the outcrop boundaries of the mountain block. In this study, the isotope data are reviewed with the aim of providing information about the water resources of the Tucson Mountains, in particular the sources and ages of the groundwater in and near the mountain block, and the nature of the aquifer or aquifers.

Background

Study Area

The topography of the Tucson Mountains is highly varied. At one extreme is craggy landscape with cliffs and steep, V-shaped canyons. At the other extreme, rolling hills surround broad sandy

or gravelly stream beds. The hard-rock outcrop of the range is surrounded by a broad, elliptical pediment consisting largely of alluvial-fan deposits. The elevation of the boundary between hard rock and the pediment ranges from 600 to 900 meters above sea level (masl), and the highest point is Wasson Peak at 1,428 masl. A semiarid to arid climate prevails. Precipitation occurs in two seasons: a season of frontal rain or snow events mainly between November and March, and a summer monsoonal season of convective rain systems between late June and September. In some years, tropical depressions bring additional rainfall in September or October. A long-term climate record is available for the Arizona-Sonora Desert Museum (ASDM) on the western flank of the range (Area D, Figure 1), where mean annual rainfall was 382 mm (69% in June-October) for 1971-2000 (Western Regional Climate Center 2020). Desert-scrub and desert-grassland vegetation types predominate (Rondeau et al. 2000).

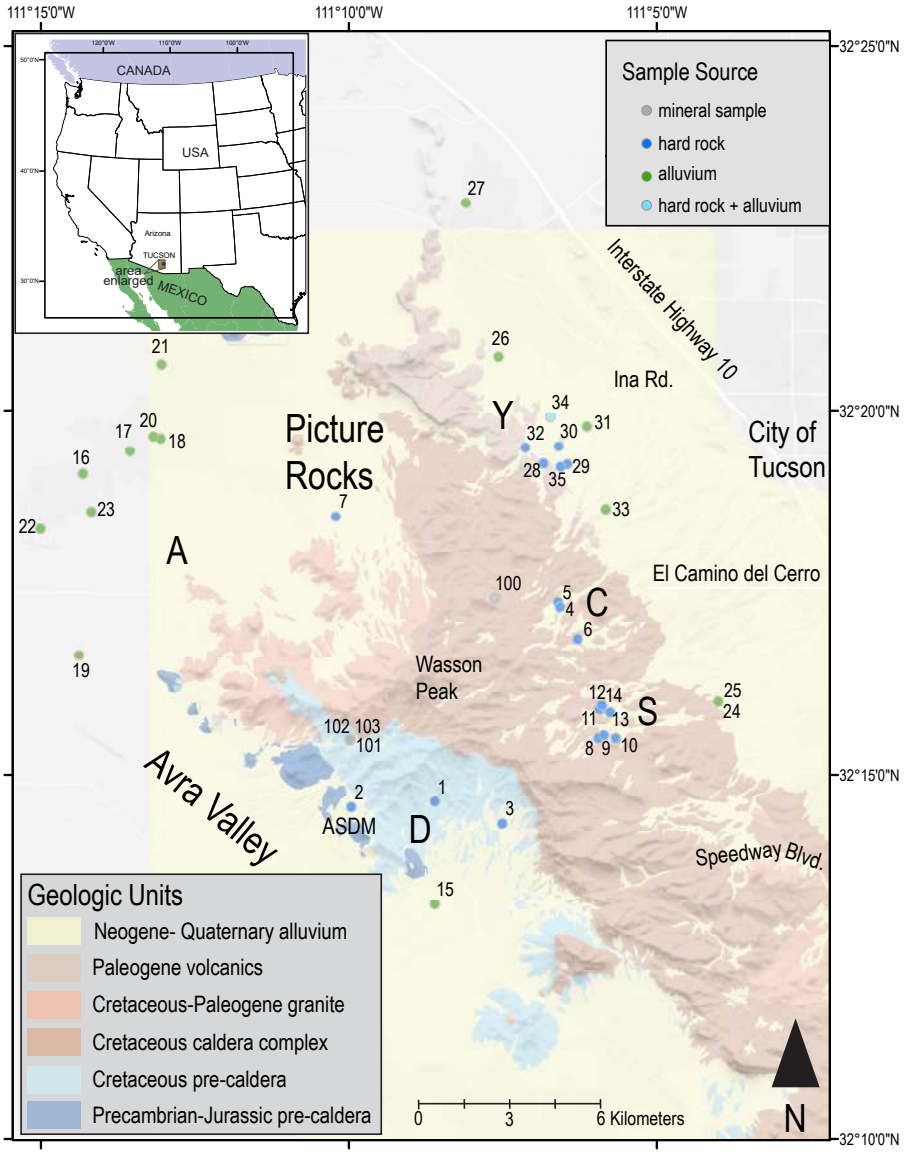

Figure 1. Map of the Tucson Mountains and surrounding area, showing geology (after Lipman 1993), and sample sites. A = Avra Valley Water Cooperative cluster; C = Camino del Cerro cluster; D = Desert Museum cluster; S = Sweetwater Drive cluster; Y = Old Yuma Mine cluster; ASDM = Arizona-Sonoran Desert Museum. Road map image is the intellectual property of Esri and is used herein under license. Copyright © 2014 Esri and its licensors. All rights reserved.

Geology

The Tucson Mountains are a fault-bounded block of crystalline rock within the Basin-and-Range Province (Fenneman 1931). The following description of the geology is from Lipman (1993) and Bezy (2005). The core of the range consists of a belt of felsic igneous rock of late Cretaceous to early Paleogene age including a supracrustal suite of rhyolitic tuff and megabreccia associated with the eruption of a large caldera, and coeval granitoids at the northwestern end of the belt. Pre-caldera units, comprising Paleozoic limestone and Mesozoic volcanic and terrestrial clastic sedimentary rocks including alluvial and minor lacustrine members, are overlain unconformably by the caldera-associated rocks along the western and southwestern flanks of the range. Post-caldera volcanic rocks of Oligocene age, mainly dacitic lava and pyroclastics, overlie the caldera rocks at the northern end of the range. Deformation of the crystalline rocks began with pre-Oligocene rotation (Hagstrum and Lipman 1991), followed by normal faulting associated with Neogene tectonic extension during the formation of the Basin-and-Range Province. Deformation has led to fracturing of the crystalline rocks.

Mineralization occurs as replacement bodies that are mainly controlled by northwest-trending fractures within late Cretaceous to early Paleogene sedimentary and volcanic rocks (Kinnison 1958). Sulfide mineralization occurs with skarn replacing thin limestone members of the Cretaceous Amole Arkose. Hypogene pyrite, galena, sphalerite, chalcopyrite, chalcocite, and molybdenite are recorded. Oxidation extends to a maximum of 13 m below the surface. In rhyolite tuff and megabreccia of the range near El Camino del Cerro, copper mineralization occurs with magnetite replacing volcanic rock. In the Old Yuma Mine, the most abundant sulfide is primary galena in a fracture zone cutting Cretaceous andesite and associated with a porphyritic dyke (Mindat.org 2020).

A broad set of alluvial fans flanks the Tucson Mountains to the east and west. The alluvial fans consist of gravel and sand transported from the mountains. The thickness of alluvium reaches 200 m within 1-2 km of the range front, according to well drillers' logs (Arizona Department of Water Resources 2020b).

Hydrogeology

Surface water is ephemeral throughout the Tucson Mountains. Springs are rare; only one spring (site 3, Figure 1) was sampled for this study. Limited information on groundwater occurrence is available in drillers' logs (Arizona Department of Water Resources 2020b). In settled areas of the mountains, groundwater is produced from domestic wells in hard rock. Available well logs provide insufficient detail to show whether water is produced from permeable strata or from fractures. In most cases, well depths are 100-200 m. Well owners in area C (Figure 1) reported declining water levels at the time of sampling. Groundwater is pumped from saturated alluvium adjacent to the mountain front, commonly from depths of 100-200 m.

Previous Work, Isotope Hydrology

Detailed studies of stable O, H, and S isotopes; tritium; and ^{14}C are available for the regional alluvial aquifer of Tucson Basin to the east of the Tucson Mountains (Eastoe et al. 2004; Gu 2005; Eastoe and Gu 2016). To the west of the range, Hess (1992) undertook a study including O and H stable isotopes in groundwater of the regional alluvial aquifer in Avra Valley. Long-term data on stable O and H isotopes in Tucson Basin precipitation were documented by Eastoe and Dettman (2016) and Wright (2001). Eastoe et al. (2011) reported a multi-year dataset for tritium in Tucson Basin precipitation. Data from these studies provided the basis for determination of isotope lapse rates in the mountain ranges surrounding Tucson Basin, and for two studies of regional recharge mechanisms. Eastoe and Towne (2018), in a study comparing recharge mechanisms of alluvial basins of the Basin-and-Range Province in Arizona, observed that basins in southern Arizona receive recharge of both summer and winter precipitation. Stable O and H isotope data are consistent with recharge occurring mainly during the wettest ~30% of months. Eastoe and Wright (2019) examined stable O and H isotope data in groundwater of mountain blocks in southern Arizona, including the Tucson Mountains. The pattern of isotope data in the Tucson Mountains is unusual in the region; the authors suggested that it represents mixing of younger and older recharge. The younger recharge

resembles a mixture of summer and winter recharge for the wettest months, like that in Tucson Basin alluvium. The older recharge appears to be ancient precipitation of late Pleistocene to early Holocene age. Beisner and Gray (2018) presented a dataset for eight wells in a small area around the Old Yuma Mine, including stable O and H isotopes in water, stable S isotopes in sulfate, tritium, and stable C isotopes and ^{14}C in dissolved inorganic carbon. They interpreted the results in terms of groundwater age.

Methods

Groundwater samples were collected from domestic supply wells in continual use. Samples were analyzed at University of Arizona and U.S. Geological Survey (USGS) laboratories.

Isotope Analytical Methods – Area Y

Stable O and H isotopes ($\delta^{18}O$ and $\delta^{2}H$) were measured at the USGS Reston Stable Isotope Laboratory in Reston, Virginia, using dual-inlet isotope ratio mass spectrometers (IRMS) on CO_2 and H_2 equilibrated at constant temperature with sample water following methods by Révész and Coplen (2008a; 2008b). The two-standard deviation (2σ) uncertainties are 0.2 per mil for $\delta^{18}O$ and 2 per mil for $\delta^{2}H$. Results are reported relative to Vienna standard mean ocean water, VSMOW. The Reston Stable Isotope Laboratory measured $\delta^{34}S$ of sulfate extracted as $BaSO_4$ from water samples. Isotope measurements were made by continuous flow IRMS on SO_2 prepared using a Carlo Erba NC 2500 elemental analyzer (Révész et al. 2012). Measurements of ^{14}C and $\delta^{13}C$ ratios were made at the National Ocean Sciences Accelerator Mass Spectrometry facility at Woods Hole Oceanographic Institution, Massachusetts, by accelerator mass spectrometry (AMS) and IRMS, respectively, on CO_2 extracted by acid hydrolysis from water samples. AMS results are reported relative to international standard Oxalic Acid I. The University of Miami Tritium Laboratory, Miami, Florida, measured tritium by gas-proportional counting on H_2 gas prepared from water samples subjected to 60-fold electrolytic enrichment, with a reporting limit of 0.3 picocurie per liter (pCi/L), or 0.1 tritium unit (TU). Measurements are standardized relative to National Institute of Standards and Technology Standard Reference Material (NIST SRM) #4926.

Isotope Analytical Methods – Other Areas

Isotopic measurements were made at the Environmental Isotope Laboratory, University of Arizona, Tucson, Arizona. $\delta^{18}O$ and $\delta^{2}H$ were measured on an automated gas-source IRMS (Finnigan Delta S). For $\delta^{2}H$ measurement, water was reacted at 750°C with Cr metal in a Finnigan H/ Device attached to the mass spectrometer. For $\delta^{18}O$ measurement, water was equilibrated with CO_2 at 15°C in an automated equilibration device coupled to the mass spectrometer. Standardization is based on international reference materials VSMOW and Standard Light Antarctic Precipitation (Coplen 1995). Analytical precision (1σ) is 0.9 ‰ or better for $\delta^{2}H$ and 0.08 ‰ or better for $\delta^{18}O$ (Eastoe and Dettman 2016). Measurements of $\delta^{34}S$ were made on $BaSO_4$ precipitated from solution at pH < 2, using a modified VG602C IRMS. Standardization is based on international standards OGS-1 and NBS123. Values of $\delta^{34}S$ are reported with an analytical precision of 0.13 ‰ (1σ). Tritium and ^{14}C were measured by liquid scintillation counting using Quantulus 1220 spectrophotometers. Tritium was measured on electrolytically enriched 0.18-L water samples, with a detection limit of 0.7 TU. Results are reported relative to NIST SRMs 4361 B and C. Dissolved inorganic carbon was extracted from 50-L water samples as $BaCO_3$, and the carbon was converted to benzene for measurement of ^{14}C. The detection limit was 0.4% modern carbon (pMC) for samples without dilution, and results are reported relative to Oxalic Acid I. Values of $\delta^{13}C$ were measured manually on CO_2 using a Finnigan Delta S mass spectrometer. The CO_2 was prepared from splits of the $BaCO_3$ extracted for ^{14}C measurement. Analytical precision was 0.1 ‰ (1σ), and measurements were calibrated using international standards NBS-19 and NBS-18.

Presentation of Data

Stable isotope measurements are expressed using δ-notation, e.g.: $\delta^{2}H = (R_{sample}/R_{standard} - 1)$ x 1000 ‰, where $R = {}^{2}H/{}^{1}H$ and the standard is VSMOW. The definitions of $\delta^{18}O$, $\delta^{34}S$, and $\delta^{13}C$ are analogous, with standards VSMOW for O,

VCDT (Vienna-Canyon Diablo Troilite) for S, and VPDB (Vienna PeeDee Belemnite) for C.

Tritium data are expressed as TU, where 1 TU = 1 atom ^{3}H per 10^{18} atoms H. Measurements of ^{14}C are expressed as pMC without normalization, where 100 pMC corresponds to the ^{14}C content of atmospheric carbon in 1950, corrected for industrial emissions.

Results

Analysis includes previously published data from Beisner and Gray (2018) and Eastoe and Wright (2019). Additionally, previously unpublished data for groundwater from the alluvium flanking the Tucson Mountains are also included in Table 1.

Stable O and H Isotopes

Values of $\delta^{18}O$ and $\delta^{2}H$ for groundwater in hard rock form a linear array with a slope near 8, distinct from and to the right of the global meteoric water line (GMWL; Figure 2). The data array is also distinct from local meteoric water lines (LMWL) defined by seasonal means for all precipitation at 1,000 masl, or by seasonal means for the wettest ~30% of months at 1,000 masl (Figure 2B). Pairs of ($\delta^{18}O$, $\delta^{2}H$) range from (-7.2, -53 ‰) to (-9.9, -75 ‰); and much of the data range is present in each of four areas with multiple samples (Figure 2A). Groundwater from alluvium immediately east and west of the Tucson Mountains mainly plots on a modified LMWL (Figure 3) defined by precipitation in the wettest ~30% of months, for 1,000 masl (an approximate mean elevation for the mountain block), with slope 6.5, or for 740 masl (a typical elevation of the boundary between the mountain-block outcrop and surrounding alluvium) with slope 6.1. Pairs of ($\delta^{18}O$, $\delta^{2}H$) range mainly from (-7.7, -54 ‰) to (-8.6, -61 ‰).

Tritium and ^{14}C

Tritium measurements range from below detection to 6.8 TU. ^{14}C measurements range from 7.8 to 101.7 pMC. Relations between $\delta^{18}O$, $\delta^{2}H$, and pMC are shown in Figures 4A and 4B. Among samples with both tritium and ^{14}C data, tritium appears generally to increase with pMC, except for groundwater in area Y, where finite tritium is found only in samples with pMC near 100 (Figure 4C).

Stable C Isotopes

Values of $\delta^{13}C$ range from -7.9 to -14.7 ‰. In area Y, but not in other areas, $\delta^{13}C$ decreases as pMC increases (Table 1). In area Y, the $\delta^{13}C$ values probably represent mixing between soil-gas CO_2, with $\delta^{13}C$ values near or below -15 ‰, and rock-carbonate sources with $\delta^{13}C > -8$ ‰. Across the study area, the latter may include Neogene pedogenic carbonate (mainly -1 to -2 ‰ in Tucson Basin alluvium, according to unpublished data of the University of Arizona Environmental Isotope Laboratory, oral communication, May 2021), Permian limestone (0 to +5 ‰; Veizer and Hoefs 1976), and Cretaceous lacustrine carbonate ($\delta^{13}C$ unknown). Soil-gas appears to predominate in groundwater with pMC near 100, drawn from Oligocene volcanic rock in area Y.

Stable S Isotopes

Values of $\delta^{34}S$ in groundwater from hard rock span a range of +0.9 to +6.9 ‰, with an outlier at +14.0 ‰ (Table 1). Two groundwater samples from alluvium, one east and one west of the range, have values of +5.3 and +5.4 ‰. These measurements are compared (Figure 5) with $\delta^{34}S$ ranges of sulfate in rainwater and dust in Tucson Basin and with Pliocene gypsum from the center of Tucson Basin (Gu 2005). Pliocene or older basin sediments may be present near the surface along the basin margins. In addition, three new measurements of $\delta^{34}S$ (+0.5, +0.6, and +1.4 ‰, on pyrite and sulfate crust from the base of a waste pile) were obtained from the Gould Mine (sites 101-103, Figure 1), where mineralization occurs as skarn replacing thin limestone lenses. A single value, +7.8 ‰, was obtained from jarositic limonite in the weathered zone at site 100.

Discussion

Recent Recharge

Values of $\delta^{18}O$ and $\delta^{2}H$ for all groundwater samples from hard rock conform to a single trend of slope near 8. Eastoe and Wright (2019) concluded that the data array represented groundwater of shorter and longer residence times, corresponding to its upper and lower ends, respectively. Addition of the data of Beisner and

Table 1. Groundwater sample data (Note: hr = hard rock; all = alluvium; m = meters; masl = meters above sea level; δ = delta, ‰, per mil; TU = tritium units; pMC = percent modern carbon).

Site number	Type	Aquifer	Date	Latitude (degrees)	Longitude (degrees)	Altitude (masl)	Depth (m)	$\delta^{18}O$ (‰)	$\delta^{2}H$ (‰)	Tritium (TU)	$\delta^{34}S$ (‰)	$\delta^{13}C$ (‰)	^{14}C (pMC)	Area (Fig. 1)
Groundwater from hard rock (Eastoe and Wright 2019)														
1	Well	hr	1999	32.244	-111.1435	871		-7.2	-53	5.4		-12.5		D
2	Well	hr	1998	32.2428	-111.1660	866	50.3	-7.2	-56	0.8		-7.9	38.9	D
3	Spring	hr	1999	32.2391	-111.1252	891	0.0	-7.9	-57	2.4		-10.7	70.0	D
4	Well	hr	7/27/2002	32.2896	-111.1102	805	150.9	-8.6	-64	<0.5	2	-8.6	33.1	C
5	Well	hr	7/27/2002	32.2885	-111.1097	828	152.4	-8.5	-62	<0.7	0.9	-10.5	28.0	C
6	Well	hr	2013	32.2812	-111.1049	825	274.4	-9.9	-75		3.4	-9.2	7.8	C
7	Well	hr	1998	32.3093	-111.1701	786	152.4	-8.1	-58	<0.7		-8.8	29.5	other
8	Well	hr	2009	32.2584	-111.0993	848	192.1	-9.4	-71			-8.6	28.4	S
9	Well	hr	2009	32.2591	-111.0978	836	122.0	-7.8	-57			-9.3	39.4	S
10	Well	hr	2009	32.2584	-111.0946	822		-8.7	-64					S
11	Well	hr	2009	32.2654	-111.0984	819	121.6	-8.6	-66					S
12	Well	hr	2009	32.2653	-111.0990	819		-7.6	-55					S
13	Well	hr	2009	32.2646	-111.0961	822	91.5	-8.7	-66					S
14	Well	hr	3/15/2003	32.2661	-111.0983	817		-8.6	-64	2.0	2.1	-10.4	53.5	S
Alluvium (Eastoe et al. 2004; previously unpublished)														
15	Well	all	5/12/1999	32.2205	-111.1435	802		-8.0	-55	1.0		-8.6	35.2	W flank
16	Well	all	11/10/1998	32.3191	-111.2385	659						-8.9	31.2	W flank
17	Well	all	11/10/1998	32.3242	-111.2258	668		-8.3	-59	<0.5	5.4			W flank
18	Well	all	11/13/1998	32.3270	-111.2175	675		-8.6	-61	<0.5				W flank
19	Well	all	10/3/1990	32.2775	-111.2396	674		-7.8	-55	<0.8		-9.1	38.0	W flank
20	Well	all	11/12/1998	32.3275	-111.2195	673		-8.5	-60	<0.6				W flank
21	Well	all	11/12/1998	32.3441	-111.2173	660		-8.5	-60	<0.6		-8.0	22.0	W flank
22	Well	all	11/12/1998	32.3065	-111.2500	656		-8.4	-59	<0.6				W flank
23	Well	all	11/12/1998	32.3104	-111.2362	673		-8.0	-57	<0.6				W flank
24	Well	all	7/21/1993	32.267	-111.0669	746	170.7	-7.6	-50	<0.7		-10.1	32.8	E flank
25	Well	all	7/13/1993	32.267	-111.0669	746	198.2	-7.7	-54	<0.7				E flank
26	Well	all	3/22/2003	32.3458	-111.1262	677	152.4	-8.4	-61	1.8	5.3	-11.0	65.0	E flank
27	Well	all	9/13/2000	32.381	-111.135	640		-8.2	-57	6.8				E flank
Old Yuma Mine area (Beisner and Gray 2018)														
28	Well	hr	01/11/16	32.32140	-111.11407	718.4	140.2	-7.6	-56	2.8	4.3	-13.9	101.7	Y
29	Well	hr	01/11/16	32.32127	-111.10762	725.7	213.4	-8.3	-63	<0.1	4.3	-11.6	49.0	Y
30	Well	hr	01/21/16	32.32528	-111.11002	710.0	118.9	-7.7	-57	<0.1	3.3	-11.9	71.9	Y
31	Well	all	01/29/16	32.32975	-111.10237	698.9	86.6	-8.2	-61	<0.1	3.4	-9.4	23.9	Y
32	Well	hr	02/08/16	32.32500	-111.11902	727.2		-7.3	-55	1.7	14.0	-14.7	99.7	Y
33	Well	all	02/09/16	32.31103	-111.09729	746.6	128.4	-8.9	-69	<0.1	6.9	-10.1	17.0	Y
34	Well	hr + all	02/29/16	32.33194	-111.11228	701.6	118.9	-7.1	-51	0.3	6.3	-9.5	40.9	Y
35	Well	hr	08/16/16	32.32068	-111.10949	723.4		-8.6	-65	<0.1	4.1	-12.1	42.2	Y

Mineral samples

Site number	Location	Latitude (degrees)	Longitude (degrees)	Mineral	$\delta^{34}S$ (‰)
100	Near Gila Monster Mine	32.2905	-111.1272	Jarosite	7.8
101	Gould Mine	32.2580	-111.1662	Sulfate crust	1.4
102	Gould Mine	32.2580	-111.1662	Pyrite	0.6
103	Gould Mine	32.2580	-111.1662	Pyrite	0.5

Gray (2018) for area Y confirms that conclusion (Figures 2A, 4A).

In both datasets, groundwater of short residence time occurs within the green ellipses of Figures 4A and 4B. Such water matches a modified LMWL defined by precipitation for the wettest ~30% of months at 1,000 masl, rather than the LMWL defined by amount-weighted seasonal mean precipitation for all months at 1,000 masl. The seasonal means are based on long-term data for 747 masl in Tucson Basin (Eastoe and Dettman 2016) and have been adjusted for altitude to 1,000 masl using isotope lapse rates from Eastoe et al. (2004). This behavior is typical of groundwater in neighboring alluvial basins, and corresponds to a regional mechanism in which recharge occurs from summer and winter precipitation during wettest months (Eastoe and Towne 2018). In the case of the Tucson Mountains, the contributions of summer precipitation are about 50 to 75%.

Groundwater with > 100 pMC or finite tritium > 1 TU or both (sites 1, 3, 14, 28, and 32; Figure 4) occurs at sites that have received recharge since 1953. Two sites (28 and 32) are wells completed in Oligocene volcanic rock, two (1 and 3) are in pre-caldera rock units in area D, and only one (14) is in the Cretaceous-early Paleogene caldera rocks in which most of the wells in areas Y, C, and S are completed. Note that the field of recent recharge (green ellipses in Figures 4A and 4B) also encompasses groundwater with pMC as low as 39, indicating that the recent recharge mechanism

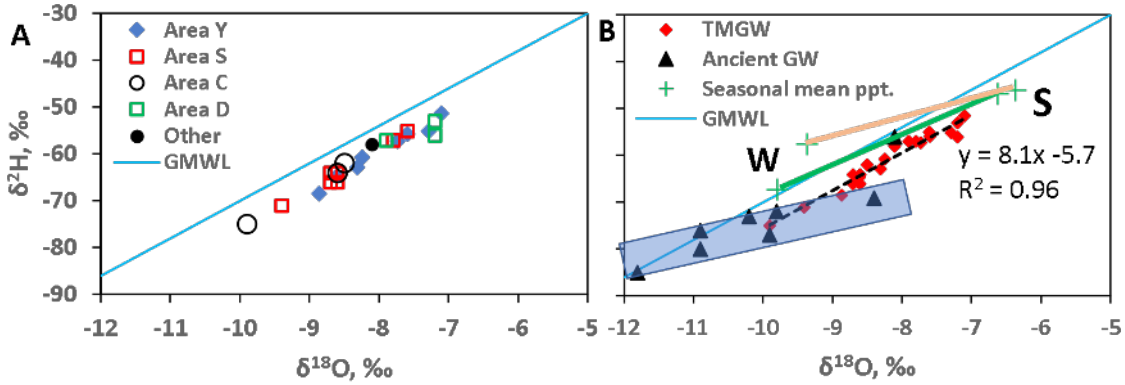

Figure 2. Plot of δ^2H vs. $\delta^{18}O$ for groundwater from the Tucson Mountains. A.) Classified by location (compare Figure 1 for cluster names). B.) In relation to mean isotope composition of seasonal precipitation at 1,000 masl, and isotope data for ancient groundwater (< 10% modern carbon) in the Tucson region (see text for data sources). TMGW = Tucson Mountains groundwater; GW = groundwater; GMWL = global meteoric water line (Craig 1961); S = summer; W = winter. Dashed line represents best fit regression line for TMGW data. Seasonal mean data with a brown tie-line are derived from data for all months in Tucson Basin; those with a green tie-line correspond to the wettest ~30% of months (Eastoe and Dettman 2016; Eastoe and Towne 2018).

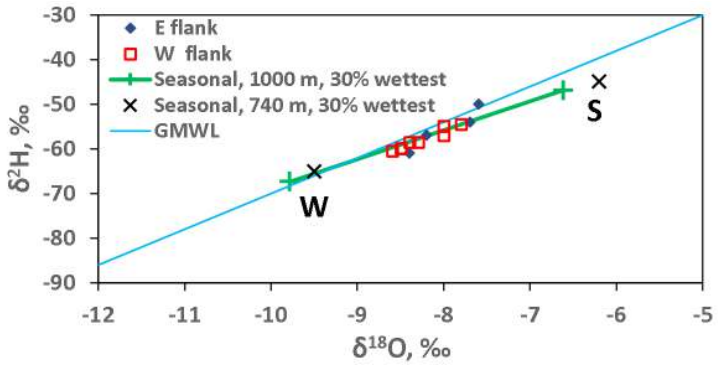

Figure 3. Plot of δ^2H vs. $\delta^{18}O$ for groundwater from wells completed in alluvium flanking the Tucson Mountains to the east (E) and west (W). Seasonal mean data for 740 and 1000 masl correspond to the wettest 30% of months (Eastoe and Dettman 2016; Eastoe and Towne 2018). GMWL = global meteoric water line (Craig 1961); S = summer; W = winter.

has operated for a considerable time, possibly thousands of years.

The number of examples is small, but these examples indicate that aquifer lithology influences the localization of recent recharge in the mountain block. Style of fracturing may play a role in enhancing recharge in certain lithologies; in addition, the type of soil profile developed on each rock type may play a role.

Residence Time of Low-$\delta^{18}O$ End Member

Beisner and Gray (2018) used criteria of Han and Plummer (2016) to establish which of their ^{14}C data could be corrected using a revised Fontes-Garnier method (Han and Plummer 2013). For instance, sample 33, containing 17 pMC, yielded corrected mean ages of 5,100 to 6700 years, the range reflecting assumptions about the pMC in dissolved rock carbonate. However, corrections of ^{14}C data using $\delta^{13}C$ as an indicator of dissolution of rock carbonate are problematic where mixing contributes to observed isotope compositions. First, mixing ratios are not accurately known. The bulk ^{14}C content, 17 pMC, might represent one of many possible mixing scenarios between older water with pMC < 17 and younger water with pMC > 17. Second, the correction equations are not constructed to account for mixing. An alternative approach to constraining the residence time of the low-$\delta^{18}O$ end member arises from its distinctive values of $\delta^{18}O$ and $\delta^{2}H$. An increase in values of $\delta^{18}O$ (typically 2 to 3 ‰) and $\delta^{2}H$ is inferred in precipitation, commonly near the end of the Pleistocene, both in southwestern North America (e.g., Phillips et al. 1986) and globally (Jasechko et al. 2015). In southern Arizona, the shift occurred between 13,000 and 15,000 years ago, on the basis of a speleothem $\delta^{18}O$ record (Wagner et al. 2010)

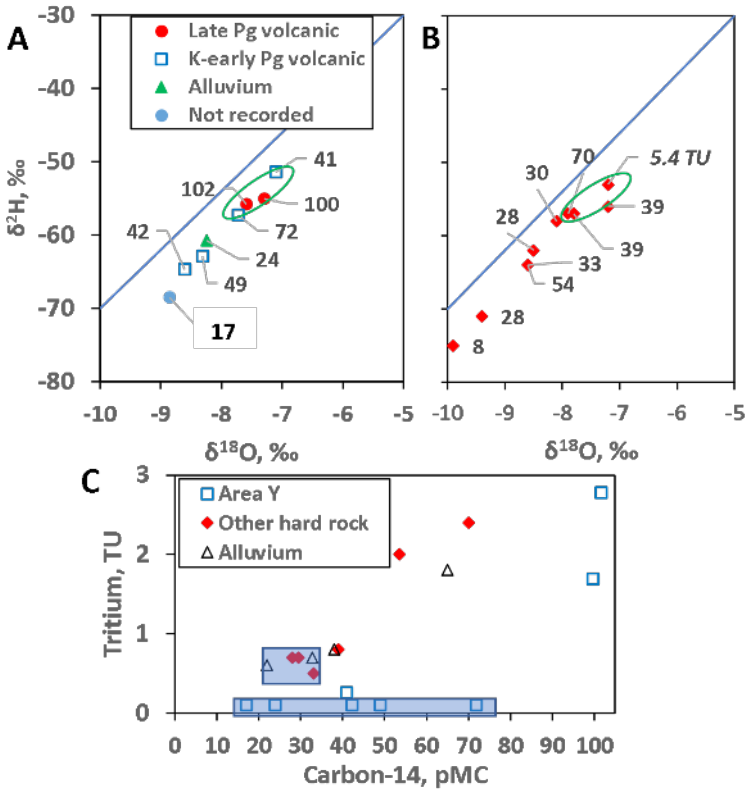

Figure 4. A.) Plot of $\delta^{2}H$ vs. $\delta^{18}O$ for groundwater from the Old Yuma Mine area (data of Beisner and Gray 2018). Data points are numbered corresponding to Figure 1 and Table 1, and classified according to the rock type in which each well was completed (records of Arizona Department of Water Resources 2020b). B.) Plot of $\delta^{2}H$ vs. $\delta^{18}O$ for groundwater from other groundwater hosted in hard rock (data of Eastoe and Wright 2019). In A and B, data points are labeled with ^{14}C content (% modern carbon, pMC, non-normalized) or tritium content (tritium units, TU), and the green ellipses indicate the field of post-bomb recharge. C.) Tritium vs. ^{14}C content in groundwater from the Tucson Mountains and flanking alluvium. Shaded blue rectangles enclose points for which tritium was below detection. For these points, the tritium value is plotted as the detection limit, 0.1 TU for area Y and 0.5-0.7 TU for other data.

from the Santa Rita Mountains, 70 km SSE of area S. The residence time of the low-$\delta^{18}O$ end member is therefore more than 13,000 years. Sample 6, with 8 pMC, falls on a broad evaporation trend (Figure 2B) defined by other ancient groundwater (< 10 pMC, uncorrected; data from Eastoe et al. 2004; Montgomery and Associates, Inc. 2009; Hopkins et al. 2014; Eastoe and Gu 2016; Tucci 2018; Schrag-Toso 2020) in the region around Tucson. Recharge of the low-$\delta^{18}O$ end member occurred from evaporated meteoric water. The seasonality of recharge in this case cannot be determined.

The presence of late Pleistocene recharge and the paucity of post-bomb recharge in most of the mountain block indicates that climate change has influenced the hydrology of the Tucson Mountains. Changes in recharge mechanism are probably related to the abundance of surface water, and may reflect climate change at the time-scale of the Holocene as indicated elsewhere in southwestern North America (Phillips et al. 1986; Wagner et al. 2010), or between the Little Ice Age and the present (discussed in a nearby study area by Eastoe 2020).

Groundwater Age, Flanking Alluvium

Most samples conform to a mixing line between mean winter and summer precipitation in the wettest months (Figure 3). A few samples contain finite tritium (sites 15, 26, and 27), indicating the presence of some post-1953 recharge. Several samples contain 22-35 pMC, indicating recharge that may be thousands of years old. The low-$\delta^{18}O$ end member discussed in the previous section is absent in the alluvium. Therefore, there is no evidence for recharge older than 13,000 years in the alluvium.

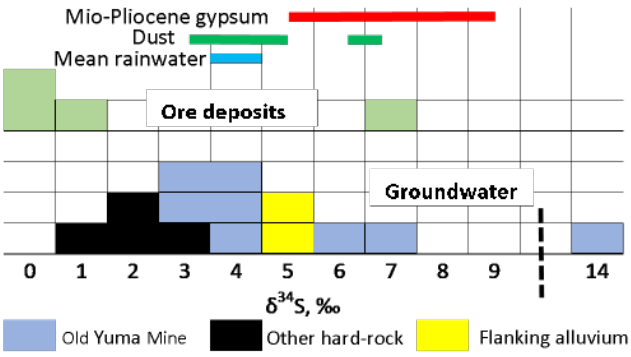

Figure 5. Frequency histogram of $\delta^{34}S$ data in groundwater and ore-related mineral samples, in relation to amount-weighted mean precipitation, dust and gypsum evaporite from central Tucson Basin (Gu 2005).

Nature of the Hard-rock Aquifer

Groundwater in the hard rock of the Tucson Mountains may reside in one or more porous strata, or in fractures with or without hydrologic connection. Groundwater with distinctive isotope compositions is closely juxtaposed in areas Y, C, and S (Figure 1). This is clearest in area S, where sites 8 ($\delta^{18}O$ = -9.4 ‰; 28.4 pMC, little dissolved Fe^{2+}) and 9 ($\delta^{18}O$ = -7.8 ‰; 39.4 pMC, containing dissolved Fe^{2+}) are about 100 m apart. Other wells, sites 10-13, within a few hundred meters of sites 8 and 9, produce water with $\delta^{18}O$ between -7.6 and -9.4 ‰. These observations are consistent with an aquifer or aquifers consisting of a poorly-connected system of fractures.

Mountain-block Recharge

At site 31 and possibly site 33, groundwater is pumped from basin-fill alluvium. At both sites, $\delta^{18}O$ and $\delta^{2}H$ data conform to the general pattern for the hard-rock aquifer (Figure 2A) and values of pMC, 33 and 17 respectively, are the lowest in area Y. Mountain-block (i.e., subsurface) recharge into alluvium is indicated near these sites. Other samples from flanking alluvium near the Tucson Mountains have a different pattern of $\delta^{18}O$ and $\delta^{2}H$ data (Figure 3), indicating that mountain-front recharge (i.e., from the surface where mountain drainages intersect the range front) predominates.

Water Quality

Groundwater from hard rock with $\delta^{34}S$ values lower than +3.5 ‰ probably contains a mixture of rain and dust sulfate with sulfate from oxidation of ore sulfide (Figure 5). Where sulfide oxidation has occurred in the hard-rock aquifer, the groundwater is also likely to contain dissolved base metals. At site 9, the well owner reported dissolved iron in the groundwater. The single sample with $\delta^{34}S$ = +14 ‰ occurs with the highest sulfate concentration, 134 ppm, in area Y (Beisner and Gray 2018). Groundwater in this well smelled of H_2S, consistent with bacterial sulfate reduction as the reason for the high $\delta^{34}S$ value.

Implications for Water Supply

Areas Y, C, and S, with low-density urban development, rely on groundwater pumped from a system of fractured-rock aquifers. The isotope evidence is consistent with little connection between fractures. Available volumes of water are therefore limited, and likely to vary from fracture to fracture. Tritium and ^{14}C data provide little evidence of replacement of groundwater by post-1953 recharge in these areas. Even if post-1953 recharge was initially present and has been removed by pumping of shallower groundwater, such water does not appear to have been replaced in recent decades. In area C (sites 4 and 5), static water levels were falling at the time of sampling based on information provided by well owners. Recharge to the mountain block under present conditions appears to be slow to non-existent. Water supply therefore appears limited, and at many sites is dependent on recharge that occurred thousands of years ago. In the absence of municipal water supply, collection of rainwater from roofs or hauling of water from elsewhere may be necessary to supplement waning groundwater supply. Capture of rainwater would have insignificant effect on recharge, given that little or no post-bomb recharge appears to be occurring in most of the mountain block.

Sustainable water supply may be possible where post-bomb replenishment of groundwater is occurring, in areas D, S, and Y. Targeted exploration, for example in the Oligocene volcanic rocks at the north end of the Tucson Mountains, may locate a renewable, but not necessarily large, water supply.

Conclusions

In the Tucson Mountains, stable O and H isotope data proved to be useful in identifying groundwater mixing and constraining groundwater residence times. Measurements of ^{14}C and tritium were useful in identifying post-bomb recharge. S isotope data helped to explain water quality issues.

Groundwater in fractured-rock aquifers in the Tucson Mountains is a mixture of recharge of different ages. Younger water, recharged since about 13,000 before the present, is a mixture of summer and winter recharge occurring during wettest months; in general, summer recharge has predominated. A similar recharge mechanism operates in alluvium flanking the range. Older groundwater has low ^{14}C content and a $\delta^{18}O$ signature consistent with recharge before 13 Ka. The seasonality of the older recharge is not known. Mountain-block recharge from fractured rock to basin alluvium occurred locally near the Old Yuma Mine. Post-bomb recharge occurs in Oligocene volcanic rock and Cretaceous sedimentary rock, but is uncommon in the Cretaceous-early Paleogene caldera complex that makes up most of the mountain block. These units might provide a renewable groundwater resource. The water-bearing fractures in the rest of the range appear to be poorly connected and receive little recharge at present. Water supply in the mountain block is therefore limited in volume, and is of variable quality where sulfide mineralization is present.

Acknowledgements

CJE acknowledges private well owners for permission to obtain samples; Jay Cole, John Schiff, and Robert Webb are thanked for help in contacting well owners; and the Environmental Isotope Laboratory at the University of Arizona is thanked for funding the analyses other than those in area Y. Analyses in area Y were funded by the U.S. Geological Survey. The authors thank two anonymous reviewers for their constructive comments. Any use of trade, firm, or product names is for descriptive purposes only and does not imply endorsement by the U.S. Government.

Author Bio and Contact Information

Christopher Eastoe (corresponding author) received his doctorate in Economic Geology from the University of Tasmania in 1979. He worked as a Staff Scientist at the University of Arizona until retirement in 2015. His research interests include the application of isotope geochemistry in studies of the hydrologic cycle, paleoclimate, and sedimentary basins. He may be contacted at eastoe@arizona.edu or Department of Geosciences, 1040 E 4th St., Room 208, Tucson, AZ 85721.

Kimberly Beisner conducts geochemical research on the evolution of groundwater from recharge through water rock interactions. She focuses on mining hydrology, dissolved gas, and isotope tracer projects throughout Arizona. Additionally, she is the USGS New

Mexico Water Science Center's Water-Quality Specialist and performs research related to understanding anthropogenic influences on the hydrologic system including emerging contaminants ranging from per- and polyflorinated compounds to wastewater tracers. She conducted aqueous chemistry undergraduate research at a Long-Term Ecological Research (LTER) prairie preserve at the University of Kansas and graduate research of selenium and trace element mobilization in the Great Salt Lake at the University of Utah. She may be contacted at kbeisner@usgs.gov or U.S. Geological Survey New Mexico Water Science Center, 6700 Edith Blvd. NE, Albuquerque, NM 87113.

References

Aishlin, P. and J.P. McNamara. 2011. Bedrock infiltration and mountain block recharge accounting using chloride mass balance. *Hydrological Processes* 25(12): 1934-1948.

Ajami, H., P.A. Troch, T. Maddock III, T. Meixner, and C. Eastoe. 2011. Quantifying mountain block recharge by means of catchment-scale storage-discharge relationships. *Water Resources Research* 47(4): W04504. DOI: 10.1029/2010WR009598.

Arizona Department of Water Resources. 2020a. *Drought Status Update*. Available at: https://new.azwater.gov/drought/drought-status. Accessed September 1, 2021.

Arizona Department of Water Resources. 2020b. *Well Registry Search*. Available at: https://gisweb.azwater.gov/WellRegistry/SearchWellReg.aspx. Accessed September 1, 2021.

Beisner, K.R. and F. Gray. 2018. *Assessment of Geochemical and Hydrologic Conditions Near Old Yuma Mine in Saguaro National Park, Arizona, 2014–17*. U.S. Geological Survey Scientific Investigations Report 2018-5019. Available at: https://doi.org/10.3133/sir20185019. Accessed December 8, 2021.

Bezy, J.V. 2005. *A Guide to the Geology of Saguaro National Park*. Arizona Geological Survey, Down to Earth Series 18, Tucson, Arizona.

Coplen, T.B. 1995. Reporting of stable carbon, hydrogen and oxygen abundances. *Proceedings of the International Atomic Energy Agency,* Vienna, Austria, 1-3 December 1993, pp. 31-34.

Craig, H. 1961. Isotopic variations in meteoric waters. *Science* 133(3465): 1702-1703.

Dwivedi, R., T. Meixner, J.C. McIntosh, P.A.T. Ferré, C.J. Eastoe, G-Y. Niu, R.L. Minor, G.A. Barron-Gafford, and J. Chorover. 2019. Hydrologic functioning of the deep critical zone and contributions to streamflow in a high-elevation catchment: Testing of multiple conceptual models. *Hydrological Proc*esses 33(4): 476-494.

Earman, S. 2004. Groundwater recharge and movement through mountain-basin systems of the Southwest: A case study in the Chiricahua Mountains-San Bernardino Valley system, Arizona and Sonora. Unpublished Dissertation, New Mexico Institute of Mining and Technology, Socorro, New Mexico, USA.

Eastoe, C.J., A. Gu, and A. Long. 2004. The origins, ages and flow paths of groundwater in Tucson Basin: Results of a study of multiple isotope systems. In: *Groundwater Recharge in a Desert Environment: The Southwestern United States*, J.F. Hogan, F.M. Phillips, and B.S. Scanlon (Eds.). American Geophysical Union, Washington, D.C., USA, pp. 217-234.

Eastoe, C.J., C.J. Watts, M. Ploughe, and W.E. Wright. 2011. Future use of tritium in mapping pre-bomb groundwater volumes. *Ground Water* 50: 87-93.

Eastoe, C.J. and R. Rodney. 2014. Isotopes as tracers of water origin in and near a regional carbonate aquifer, the southern Sacramento Mountains, New Mexico. *Water* 6(2): 301-323.

Eastoe, C.J. and D.L. Dettman. 2016. Isotope amount effects in hydrologic and climate reconstructions of monsoon climates: Implications of some long-term data sets for precipitation. *Chemical Geology* 430: 76-89.

Eastoe, C.J. and A. Gu. 2016. Groundwater depletion beneath downtown Tucson, Arizona: A 240-year record. *Journal of Contemporary Water Research and Education* 159: 62-77.

Eastoe, C.J. and D. Towne. 2018. Regional zonation of groundwater recharge mechanisms in alluvial basins of Arizona: Interpretation of isotope mapping. *Journal of Geochemical Exploration* 194: 134-145.

Eastoe, C.J. and W.E. Wright. 2019. Hydrology of mountain blocks in Arizona and New Mexico as revealed by isotopes in groundwater and precipitation. *Geosciences* 9(11): 461. DOI: 10.3390/geosciences9110461.

Eastoe, C.J. 2020. Sources of perennial water supporting critical ecosystems, San Pedro Valley, Arizona. *Environmental and Engineering Geoscience* 26: 463-479.

Fenneman, N.M. 1931. *Physiography of Western United States*. McGraw Hill, New York, NY, USA.

Gabrieli, C.P., J.J.. McDonnell, and W.T. Jarvis. 2012. The role of bedrock groundwater in rainfall-runoff response at hillslope and catchment scales. *Journal of Hydrol*ogy 450-451: 117-133.

Gu, A. 2005. Stable isotope geochemistry of sulfate in groundwater of southern Arizona: Implications for groundwater flow, sulfate sources, and environmental significance. Unpublished Dissertation, University of Arizona, Tucson, Arizona, USA.

Hagstrum, J.T. and P.W. Lipman. 1991. Late Cretaceous paleomagnetism of the Tucson Mountains: Implications for vertical axis rotations in south central Arizona. *Journal of Geophysical Research* 96(B10): 16069-16081.

Han, L.-F. and L.N. Plummer. 2013. Revision of Fontes & Garnier's model for the initial ^{14}C content of dissolved inorganic carbon used in groundwater dating. *Chemical Geology* 351: 105-114.

Han, L.-F. and L.N. Plummer. 2016. A review of single-sample-based models and other approaches for radiocarbon dating of dissolved inorganic carbon in groundwater. *Earth-Science Reviews* 152: 119-142.

Harris, C., C. Burgers, J. Miller, and F. Rawoot. 2010. O- and H-isotope record of Cape Town rainfall from 1996 to 2008, and its application to recharge studies of Table Mountain groundwater, South Africa. *South African Journal of Geology* 113(1): 33-56.

Hess, G.S. 1992. Chemical and isotopic evidence for irrigation return flow in Avra Valley, Arizona. Unpublished Thesis, University of Arizona, Tucson, Arizona.

Hopkins, C., J. McIntosh, J. Dickinson, C. Eastoe, and T. Meixner. 2014. Evaluation of the importance of clay confining units on groundwater flow in alluvial basins using solute and isotope tracers: The case of Middle San Pedro Basin in southeastern Arizona (USA). *Hydrogeology Journal* 22: 829-849.

James, E.R., M. Manga, T.P. Rose, and G.B. Hudson. 2000. The use of temperature and the isotopes of O, H, C, and noble gases to determine the pattern and spatial extent of groundwater flow. *Journal of Hydrology* 237: 100-112.

Jasechko, S., A. Lechler, F.S.R. Pausata, P.J. Fawcett, T. Gleeson, D.I. Cendón, J. Galeewsky, A.N. LeGrande, C. Risi, Z.D. Sharp, J.M. Welker, M. Werner, and K. Yoshimura. 2015. Late-glacial to late-Holocene shifts in global precipitation $\delta^{18}O$. *Climate of the Past* 11(10): 1375-1393.

Kalin, R.M. 1994. The hydrogeochemical evolution of the groundwater of the Tucson Basin with application to 3-dimensional groundwater flow modeling. Unpublished Dissertation, University of Arizona, Tucson, Arizona, USA.

Katsuyama, M., N. Ohte, and N. Kabeya. 2005. Effects of bedrock permeability on hillslope and riparian groundwater dynamics in a weathered granite catchment. *Water Resources Res*earch 41(1): W01010. DOI: 10.1029/2004WR003275.

Kinnison, J.E. 1958. Geology and ore deposits of the southern section of the Amole mining district, Tucson Mountains, Pima County, Arizona. Unpublished Thesis, University of Arizona, Tucson, Arizona.

Lipman, P.W. 1993. Geologic Map of the Tucson Mountains Caldera, Southern Arizona. United States Geological Survey Miscellaneous Investigations Series Map I-2205, scale 1:24,000.

Manning, A.H. and D.K. Solomon. 2004. Constraining mountain-block recharge in eastern Salt Lake Valley, Utah with dissolved noble gas and tritium data. In: *Groundwater Recharge in a Desert Environment: The Southwestern United States*, J.F. Hogan, F.M. Phillips, and B.S. Scanlon (Eds.). American Geophysical Union, Washington, D.C., USA, pp. 139-158.

Mindat.org. 2020. Old Yuma Mine (Yuma Mine). Available at: https://www.mindat.org/loc-3372.html. Accessed September 1, 2021.

Montgomery, E.L. and Associates, Inc. 2009. *Results of Phase 2 Hydrogeologic Investigations and Monitoring Program, Rosemont Project, Pima County, Arizona*. Report prepared for Rosemont Copper Company, Tucson, Arizona. Available at: https://www.rosemonteis.us/documents/012065. Accessed September 1, 2021.

Newton, B.T., G.C. Rawling, S.S. Timmons, L. Land, P.S. Johnson, T.J. Kludt, and J.M. Timmons. 2012. *Sacramento Mountains Hydrogeology Study*. New Mexico Bureau of Geology and Mineral Resources Open-file Report 543. Available at: https://geoinfo.nmt.edu/publications/openfile/downloads/500-599/543/OFR-543_HR.pdf. Accessed December 8, 2021.

Phillips, F.M., L.A Peeters, M.K. Tansey, and S.N. Davis. 1986. Paleoclimatic inferences from an isotopic investigation of groundwater in the central San Juan Basin, New Mexico. *Quaternary Research* 26(2): 179-193.

Ren, S., A.D. Parsekian, Y. Zhang, and B.J. Carr. 2019. Hydraulic conductivity calibration of logging NMR in a granite aquifer, Laramie Range, Wyoming. *Groundwater* 57(2): 303-319.

Révész, K. and T.B. Coplen. 2008a. *Determination of the $\delta(^2H/^1H)$ of Water: RSIL Lab Code 1574*. U.S. Geological Survey Techniques and Methods 10-C1. Available at: https://doi.org/10.3133/tm10C1. Accessed December 8, 2021.

Révész, K. and T.B. Coplen. 2008b. *Determination of the $\delta(^{18}O/^{16}O)$ of Water: RSIL Lab Code 489*. U.S. Geological Survey Techniques and Methods 10-C2. Available at: https://pubs.usgs.gov/tm/2007/tm10c2/pdf/tm10c2.pdf. Accessed December 8, 2021.

Révész, K., H. Qi, and T.B. Coplen. 2012. *Determination of the $\delta^{34}S$ of Sulfate in Water; RSIL Lab Code 1951*. U.S. Geological Survey Techniques and Methods 10-C10. Available at: https://pubs.usgs.gov/tm/2007/tm10c2/pdf/tm10c2.pdf. Accessed December 8, 2021.

Rondeau, R.J., T.R. Van Devender, C.D. Bertelsen, P.D. Jenkins, R.K. Van Devender, and M.A. Dimmitt. 2000. Flora and Vegetation of the Tucson Mountains, Pima County, Arizona. The University of Arizona Herbarium, Tucson, Arizona. Available at: https://cals.arizona.edu/herbarium/content/flora-and-vegetation-tucson-mountains-pima-county-arizona. Accessed September 1, 2021.

Schrag-Toso, S.C. 2020. *Isotopes, Geochemistry, Citizen Science and Local Partnerships as Tools to Build Upon a Fractured Understanding of the Hydrology of the Patagonia Mountains*. Climate Assessment of the Southwest Climate and Society Fellowship Final Report. University of Arizona, Tucson, Arizona.

Thiros, S.A. and A.H. Manning. 2004. *Quality and Sources of Ground Water Used for Public Supply in Salt Lake Valley, Salt Lake County, Utah, 2001*. U.S. Geological Survey Water-Resources Investigations Report 2003-4325. DOI: 10.3133/wri034325.

Tucci, R.S. 2018. Using isotopes and solute tracers to infer groundwater recharge and flow in the Cienega Creek watershed, SE Arizona. Unpublished Thesis, University of Arizona, Tucson, Arizona.

Udall, B. and J. Overpeck. 2017. The twenty-first century Colorado River hot drought and implications for the future. *Water Resources Research* 53(3): 2404-2418. DOI: 10.1002/2016WR019638.

United States Global Climate Research Program (USGCRP). 2017. *Climate Science Special Report: Fourth National Climate Assessment (NCA4), Volume I*. Washington, D.C. Available at: http://doi.org/10.7930/J0J964J6. Accessed December 8, 2021.

Veizer, J. and J. Hoefs. 1976. The nature of O^{18}/O^{16} and C^{13}/C^{12} secular trends in sedimentary carbonate rocks. *Geochimica et Cosmochimica Acta* 40(11): 1387-1395.

Wagner, J.D.M., J.E. Cole, J.W. Beck, P.J. Patchett, G.M. Henderson, and H.R. Barnett. 2010. Moisture variability in the southwestern United States linked to abrupt glacial climate change. *Nature Geoscience* 3: 110-113.

Wahi, A.K., J.F Hogan, B. Ekwurzel, M.N. Baillie, and C.J. Eastoe. 2008. Geochemical quantification of semiarid mountain recharge. *Ground Water* 46(3): 414-425.

Welch, L.A. and D.M. Allen. 2012. Consistency of groundwater flow patterns in mountainous topography: Implications for valley bottom water replenishment and for defining groundwater flow boundaries. *Water Resources Research* 48(5): W05526. DOI: 10.1029/2011wr010901.

Welch, L.A. and D.M. Allen. 2014. Hydraulic conductivity characteristics in mountains and implications for conceptualizing bedrock groundwater flow. *Hydrogeology Journal* 22(5): 1003-1026.

Western Regional Climate Center. 2020. Arizona. Available at: http://www.wrcc.dri.edu/summary/Climsmaz.html. Accessed September 1, 2021.

Wilson, J.L. and H. Guan. 2004. Mountain-block hydrology and mountain-front recharge. In: *Groundwater Recharge in a Desert Environment: The Southwestern United States*, J.F. Hogan, F.M. Phillips, and B.S. Scanlon (Eds.). American Geophysical Union, Washington, D.C., USA, pp. 113-138.

Winograd, I.J., A.C. Riggs, and T.B. Coplen. 1998. The relative contributions of summer and cool-season precipitation to groundwater recharge, Spring Mountains, Nevada, USA. *Hydrogeology Journal* 6(1): 77-93.

Wright, W.E. 2001. δD and $\delta^{18}O$ in mixed conifer systems in the U.S. Southwest: The potential of $\delta^{18}O$ in *Pinus ponderosa* tree rings as a natural environmental recorder. Unpublished Dissertation, University of Arizona, Tucson, Arizona, USA.